Geophysical Research Letters

RESEARCH LETTER
10.1029/2022GL098041

Spaceborne Evidence That Ice-Nucleating Particles Influence High-Latitude Cloud Phase

Tim Carlsen[1] and Robert O. David[1]

[1]Department of Geosciences, University of Oslo, Oslo, Norway

T. Carlsen and R. O. David contributed equally to this work.

Key Points:

- Ice-nucleating particles (INPs) control ice formation in high-latitude clouds
- Sea ice and snow cover inhibit the local emission of INPs, which directly influences cloud phase in the Arctic and Southern Ocean
- This has implications for the predicted negative cloud phase feedback with future warming and the associated sea ice and snow cover loss

Supporting Information:

Supporting Information may be found in the online version of this article.

Correspondence to:

T. Carlsen and R. O. David,
tim.carlsen@geo.uio.no;
r.o.david@geo.uio.no

Citation:

Carlsen, T., & David, R. O. (2022). Spaceborne evidence that ice-nucleating particles influence high-latitude cloud phase. *Geophysical Research Letters*, *49*, e2022GL098041. https://doi.org/10.1029/2022GL098041

Received 24 JAN 2022
Accepted 23 JUN 2022

© 2022 The Authors.
This is an open access article under the terms of the Creative Commons Attribution-NonCommercial License, which permits use, distribution and reproduction in any medium, provided the original work is properly cited and is not used for commercial purposes.

Abstract Mixed-phase clouds (MPCs), which consist of both supercooled cloud droplets and ice crystals, play an important role in the Earth's radiative energy budget and hydrological cycle. In particular, the fraction of ice crystals in MPCs determines their radiative effects, precipitation formation and lifetime. In order for ice crystals to form in MPCs, ice-nucleating particles (INPs) are required. However, a large-scale relationship between INPs and ice initiation in clouds has yet to be observed. By analyzing satellite observations of the typical transition temperature (T*) where MPCs become more frequent than liquid clouds, we constrain the importance of INPs in MPC formation. We find that over the Arctic and Southern Ocean, snow and sea ice cover significantly reduces T*. This indicates that the availability of INPs is essential in controlling cloud phase evolution and that local sources of INPs in the high-latitudes play a key role in the formation of MPCs.

Plain Language Summary Mixed-phase clouds (MPCs), which consist of both liquid droplets and ice crystals, play an important role for the Earth's climate system. For example, the number of ice crystals in MPCs determines how much sunlight is reflected by the cloud and how efficiently the cloud can form precipitation. The formation of ice crystals in MPCs requires a special subset of aerosol particles called ice-nucleating particles (INPs). INPs are required for liquid cloud droplets to freeze at temperatures warmer than −36°C. However, a large-scale relationship between INPs and ice formation in clouds has yet to be observed. Using satellite observations, we determine the transition temperature (T*) where MPCs become more frequent than liquid clouds and find that T* is strongly dependent on snow and sea ice cover over the Arctic and Southern Ocean. This indicates that sea ice and snow cover act as a lid that inhibits the emission of INPs from the ocean. In a warming world with retreating sea ice and snow cover, our results suggest that clouds in these regions will contain ice crystals at warmer temperatures than previously estimated and, thus, have potential implications for future warming predictions.

1. Introduction

The amount of liquid and ice within mixed-phase clouds (MPCs) influences precipitation formation, cloud lifetime, and electrification (Cantrell & Heymsfield, 2005). Simultaneously, the thermodynamic phase composition controls the radiative properties of MPCs due to the different scattering properties between liquid water and ice. In a warming climate, MPCs are believed to transition toward a state with more liquid water and a higher albedo, which limits future warming (Bjordal et al., 2020; Zelinka et al., 2020). This cloud phase feedback makes the accurate representation of ice crystal concentrations in MPCs in Earth System Models essential for correctly predicting the future climate (Forster et al., 2021; Tan et al., 2016). But what controls the formation of ice and the thermodynamic phase composition in MPCs?

The importance of ice-nucleating particles (INPs) for forming ice in MPCs is undisputed. Laboratory experiments show that pure water does not freeze without the presence of an INP until it is supercooled to around −36°C. Therefore, field measurements including precipitation sampling (Petters & Wright, 2015; Vali, 1971), airborne (Borys, 1989; DeMott et al., 2010; Pratt et al., 2009; Rogers et al., 2001), ship (Welti et al., 2020; Wilson et al., 2015), and mountaintop measurements (Lacher et al., 2017) have been conducted to investigate the abundance of INPs, globally. These studies have found that INP concentrations can vary by several orders of magnitude at a given temperature. This variability is partially explained by the location and type of aerosol acting as INPs (Kanji et al., 2017). Close to the Earth's major deserts, dust is the primary source of INPs, especially at temperatures below −15°C (Atkinson et al., 2013; Boose et al., 2016; Murray et al., 2012). Meanwhile, in more remote regions and at higher temperatures, biological sources such as sea spray aerosol are believed to be

the most important source of INPs (Burrows et al., 2013; McCluskey et al., 2018; Schnell & Vali, 1975; Wilson et al., 2015; Irish et al., 2019).

Based on the fundamental importance of INPs for ice crystal formation in MPCs, INP parametrizations have been developed to account for different aerosol species and the observed variability from field and laboratory studies. When implemented into Earth System Models, different INP parametrizations can have profound effects on both MPC optical properties and lifetimes. However, when in situ ice crystal number concentrations are compared with INP concentrations, they seldomly agree (Mignani et al., 2019) and ice crystal concentrations often exceed INP concentrations by several orders of magnitude (Ladino et al., 2017; Rangno & Hobbs, 2001; Ramelli et al., 2021). This would suggest that INPs are not as important for ice crystal formation in naturally occurring MPCs. The main explanation for this discrepancy is secondary ice production (SIP; Hallett & Mossop, 1974; Korolev & Leisner, 2020), which has been shown to rapidly increase the concentration of ice crystals in MPCs through what has been described as a cascading process (Lawson et al., 2015). Nevertheless, the occurrence and efficiency of secondary ice processes is still an area of open research.

Another and larger scale approach to assess the influence of INPs on MPCs has been through the so-called supercooled liquid fraction (ratio of supercooled liquid to ice). The supercooled liquid fraction and ambient aerosol concentration (a proxy for INPs) comparisons show that there is a spatial correlation, but a weak dependence between dust aerosols and the supercooled liquid fraction of MPCs at a given temperature (Choi et al., 2010; Tan et al., 2014). However, the supercooled liquid fraction is prone to the influence of dynamics (vertical velocities), the Wegener-Bergeron-Findeisen process (Korolev, 2007), and secondary ice processes, thereby masking the importance of INPs for the distribution of the cloud phase.

Therefore, with the exception of laboratory and modeling studies, direct evidence of the importance of INPs on MPC formation and subsequent thermodynamic phase composition has yet to be observed or quantified. Here we show that by using the transition temperature from supercooled liquid clouds to MPCs, as observed by satellites, the influence of INPs on the thermodynamic phase composition in MPCs can be assessed. In particular, we focus this analysis on the high-latitudes, where MPCs are abundant (Korolev et al., 2017). To take into account that ice nucleation occurs within the liquid layer near the top of MPCs (Morrison et al., 2012), we further restrict our analysis to liquid-top MPCs (LTMPCs). This is in accordance with de Boer et al. (2010) and Westbrook and Illingworth (2013), who found that liquid clouds are a prerequisite for primary ice nucleation in high-latitude MPCs. Additionally, field studies indicate that local INP emissions have a strong seasonal dependence in the Arctic (Tobo et al., 2019; Wex et al., 2019), providing a unique opportunity to analyze the influence of differing INP concentrations on MPCs. We find that this transition temperature is significantly suppressed over sea ice and snow, suggesting that INPs play a critical role in the evolution of cloud phase and that the INPs in this region are primarily of a local nature.

2. Materials and Methods

Here we use satellite observations from CloudSat (Stephens et al., 2002) and the Cloud-Aerosol Lidar and Infrared Pathfinder Satellite Observation (CALIPSO, Winker et al., 2010) to discriminate between single-layer liquid only (LO) and LTMPCs and combine them with cloud top temperatures (CTTs) from atmospheric reanalysis data to characterize the occurrence of both cloud types as a function of CTT (see Figures 1a and 1b). The warmest CTT when LTMPCs become more frequent than LO clouds, is hereafter referred to as T* (see Figure 1c). We perform this analysis on a $5° \times 5°$ grid (see Figure 1d) for each season over nine years (2006–2017). Here we use the CTT instead of the coldest temperature in the cloud as ice precipitation has been observed to fall from cloud top even in clouds that extend into an inversion or occur during warm air events (Achtert et al., 2020). In this section, the calculation of T*, its significance, and the averaging procedure are described together with the processing of the sea ice data used in the interpretation of the results.

2.1. Satellite Data and Definition of Cloud Regimes

For the discrimination between LO clouds and LTMPCs, we use the data product 2B-CLDCLASS-LIDAR (Sassen et al., 2008), which combines observations from the cloud profiling radar on CloudSat (Stephens et al., 2002) and the Cloud-Aerosol Lidar with Orthogonal Polarization (CALIOP) (Winker et al., 2007) on CALIPSO (Winker et al., 2010). The 2B-CLDCLASS-LIDAR product utilizes the different sensitivities of the radar and lidar to liquid

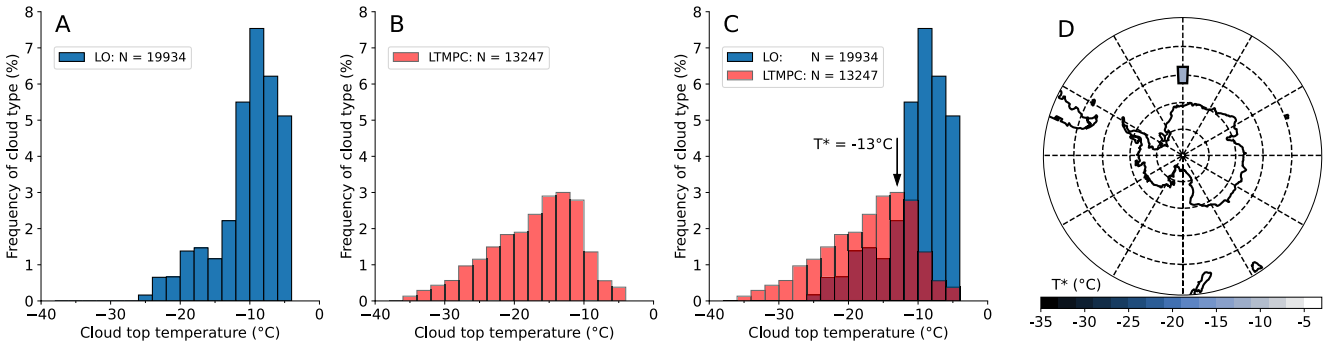

Figure 1. Frequency of cloud types (in %) with respect to cloud top temperature (bin width: 2°C) for the 5° × 5° grid cell centered at 60°S and 0°E combining nine austral summer seasons (DJF, 2006–2009 and 2012–2016). (a) for liquid-only (LO) clouds, (b) for liquid-top MPCs (LTMPCs), (c) The combination of LO and LTMPC frequency distributions yields an exemplary T* of −13°C. (d) Visualization of the 5° × 5° grid cell used for cloud type analysis in Figures 1a–1c. *N* denotes the number of observations within the grid cell of the respective cloud types.

droplets and ice crystals to determine the phase of a cloud layer. The logics of the phase determination algorithm are based on a temperature dependent radar reflectivity threshold (Zhang et al., 2010), the integrated attenuated lidar backscattering coefficient, and cloud base and top temperatures from atmospheric reanalysis (Wang, 2019). This way, each individual cloud layer of the radar profile gets assigned a phase (variable `CloudPhase`: "ice", "mixed", or "water"). Here we restrict our analysis to single-layer clouds in order to exclude the possibility of ice falling from aloft into the clouds of interest. The cloud phase information comes with a confidence level assigned to the cloud phase (variable `CloudPhaseConfidenceLevel`). The confidence value generally ranges from 0 to 10, where 10 indicates the highest confidence level. While it is not recommended to use data with a confidence level of five or lower, we further restrict our analysis to cloud phase confidence levels of seven or higher. For each cloudy profile, we retrieve the CTT from the ECMWF-AUX data set that contains ancillary European Centre for Medium-Range Weather Forecast (ECMWF) state variable data interpolated to each vertical radar bin. For the definition of the different cloud types, we include observations with CTTs below −3°C to stay away from the temperature limits of the phase determination algorithm. We define LO clouds and MPCs based on the `CloudPhase` variable of "water" or "mixed", respectively. For the definition of LTMPCs, we further use the `Water_layer_top` variable from the 2B-CLDCLASS-LIDAR product, which indicates the location of a possible water layer in MPCs. We define LTMPCs as all MPCs where the `Water_layer_top` is within three vertical radar bins (90 m) of the cloud top height (variable `CloudLayerTop`). The CTT of all LO and LTMPCs are combined into 5° × 5° grid cells over the entire globe. Then the CTTs of the LO and LTMPCs are binned into 2°C temperature bins by season for the years 2006–2017.

For each 5° × 5° grid cell, the LO and LTMPC observations are normalized by the total number of single-layer observations (LO, MPCs, ice-only) in the given cell. Finally, T* is then defined as the warmest CTT bin, where LTMPCs are more frequent than LO clouds and where at least 10 LTMPCs were observed within that given season summed over the nine-year period.

2.2. Significance of T*

To test the robustness and significance of T*, its calculation is repeated 100 times using random sampling with replacement (bootstrapping) of the original observations of both LO and LTMPCs for each grid cell and each season. The significance of T* is estimated based on the distribution of the T* values from the bootstrapped calculations by calculating the standard error (SE) from the standard deviation σ of the bootstrapped T* and the number of bootstrapped T* values (100):

$$\mathrm{SE} = \frac{\sigma}{\sqrt{100}} \tag{1}$$

From the SE, the 99% confidence interval (CI) can be calculated as:

$$\mathrm{CI} = 2.58 \cdot \mathrm{SE} \tag{2}$$

Table 1
Area-Weighted Averages of Significant T (in °C) for Different Regions and Seasons*

	Ocean	Land	Sea ice
Arctic			
Summer (JJA)	−13	−14	-
Winter (DJF)	−17	−23	−24
Southern Ocean			
Summer (DJF)	−14	-	-
Winter (JJA)	−17	-	−27

Note. The masks used for averaging are displayed in Figure S2 in Supporting Information S1.

Grid cells are classified as insignificant if the CI is larger than 0.5°C (corresponding to a T* confined to about 1 bin during bootstrapping) and are excluded from the analysis. Most grid cells analyzed within this study show very robust T* values (see Figure S1 in Supporting Information S1).

For the difference in T* (Summer to Winter) in Figures 2c and 2f, the grid cells where the sum of the summer and winter CIs is larger than the absolute value of the T* difference (min/max error propagation) are treated as insignificant.

2.3. Sea Ice Data

The sea ice concentration data is from the Institute of Environmental Physics (IUP), University of Bremen, based on the ARTIST Sea Ice (ASI) algorithm (Spreen et al., 2008). The ASI retrieval is applied to microwave radiometer data of the AMSR-E (Advanced Microwave Scanning Radiometer for EOS) on the Aqua satellite and AMSR2 (Advanced Microwave Scanning Radiometer 2) on GCOM-W1 sensors, which were reprocessed in 2018 for both platforms with the same parameters. The sea ice edge as visible in Figure 2 is calculated using the following steps: (a) Retrieval of the dates for the Arctic/Antarctic sea ice maximum/minimum for each year (Grosfeld et al., 2016) and calculation of the multi-year average of the sea ice maxima/minima from these days. If the maximum/minimum occurred in March/September, we used the last day of the respective season (February/August) in the calculation. (b) The sea ice edge is defined where the sea ice concentration is at least 15%. (c) Re-gridding of the sea ice data on a regular 0.25° × 0.25° grid using bilinear interpolation.

2.4. Averaging of T*

We perform area-weighted averaging of T* for the different regions and seasons based on the sea ice concentrations and land/ocean masks (from ASI data set) that we re-gridded on the 5° × 5° grid of T* using bilinear interpolation. Further, grid cells with insignificant T* values are excluded from the averaging. The resulting masks used for the calculation of the average T* values in Table 1 are displayed in Figure S2 in Supporting Information S1.

3. Results and Discussion

T* is based on the underlying principle that as the CTT of LO clouds cool, the initiation of ice becomes more likely as a larger fraction of aerosols can act as INPs (Fletcher, 1962; Meyers et al., 1992) and therefore, the probability of observing LTMPCs increases. As shown by the exemplary histograms in Figure 1, the observed frequency of LTMPCs increases at colder temperatures, as expected, and exceeds that of LO clouds at −13°C. Therefore, in this example the T* of −13°C represents the typical temperature at which INPs act to alter the cloud phase for this region.

When calculating T* over the Arctic as a function of sea and land mask (see Table 1), we find that during the summer time (JJA), T* is −13°C over the ocean and −14°C over land (Figure 2a). At these temperatures, biological INPs are expected to be dominant (Kanji et al., 2017) and indeed field studies have shown that INPs are primarily biological during the Arctic summer (Creamean et al., 2019; Tobo et al., 2019). T* is homogeneous over both the land and the ocean and this suggests that the abundance of INPs and their efficiency is rather similar throughout the region. The only exception is over the Greenland ice sheet (lower T* values, see Figure 2a) where due to its high altitude and frequently cold temperatures, INPs are expected to be washed out during transport to this area (Stopelli et al., 2015) or relatively INP-depleted air from the free troposphere (Lacher et al., 2018) descends over the ice sheet (Guy et al., 2021). Consistently, field measurements have shown that INP concentrations are lower over the Greenland ice sheet than elsewhere during the Arctic summertime (Wex et al., 2019).

In contrast, during the winter months (DJF) the T* over the sea ice region (green line in Figure 2) drops to −24°C, while over open ocean it slightly decreases to −17°C (Figure 2b, compare Table 1). Similarly, during the winter months snow cover reduces T* to −23°C over land. This temperature is consistent with the typical freezing temperature of dust (e.g., Murray et al., 2012), which could be transported into the Arctic during air

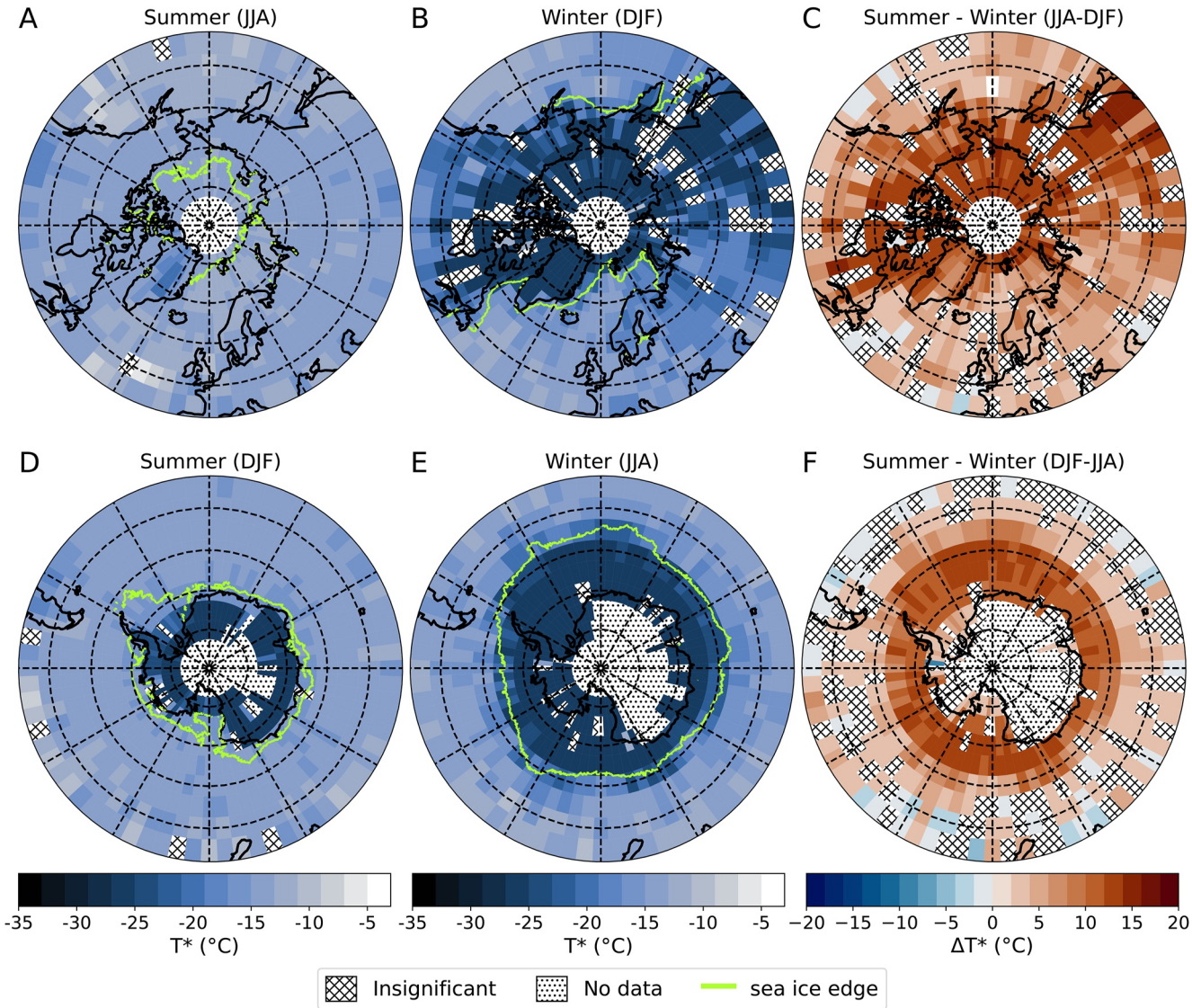

Figure 2. Seasonal T* over the Arctic and the Southern Ocean based on observations between 2006 and 2017. Grid cells where T* calculations are insignificant (on a 99% confidence level) are hatched, while dotted areas have no data. The green line shows the average minimum/maximum sea ice edge between 2006 and 2017, defined as the 15% sea ice concentration line for the given season. Arctic T* during Summer (JJA), Winter (DJF) and the difference between Summer and Winter (Summer minus Winter) are shown in panel (a–c), respectively. Similarly, the Southern Ocean T* during Austral Summer (DJF), Winter (JJA) and the difference between Summer and Winter (Summer minus Winter) are shown in panel (d–f), respectively.

mass intrusions (Engelmann et al., 2021; Pithan et al., 2018). Fountain and Ohtake (1985) found that seasonal INP concentrations in Alaska were dominated by local sources with occasional episodes of high concentrations associated with long-range transported dust. Thus, the largest seasonal differences in T* are observed in regions covered by snow and sea ice during the winter, when no local biogenic INP sources are available (Figure 2c). Previous ship (Bigg, 1996; Bigg & Leck, 2001) and coastal (Creamean et al., 2018) measurements also observed a dependence of the INP concentration on the extent of snow and sea ice coverage, with a decrease and increase in INP concentration during the Fall freeze up and Spring thaw, respectively. A reduction in wintertime INP concentration was also observed at an inland Arctic location in Alaska (Borys, 1983) and a Boreal Forest in Finland (Schneider et al., 2021). Similarly, Wex et al. (2019) observed an increase in INPs during the snow-free summer months and a decrease during the winter months at four different measurement locations in the Arctic. Their back trajectory analysis showed that the highest INP concentrations were associated with air mass interaction with snow-free terrain and open water, while the lowest concentrations came from the sea ice and snow.

Airborne Arctic INP measurements (Borys, 1989; Hartmann et al., 2020) also observed a decrease in INP concentration over sea ice and snow cover. The only exception was over open leads in the sea ice (Curry et al., 2000; Hartmann et al., 2020; Rogers et al., 2001), which further indicates that sea ice inhibits the emission of INPs. This lack of available biological INPs has also been used to explain the lower temperatures required to observe MPCs in the Arctic relative to the midlatitudes and tropics (Costa et al., 2017). Furthermore, Griesche et al. (2021) observed a decrease in the frequency of ice containing clouds when they were decoupled from the ocean surface, also indicating that marine INPs are essential for ice formation in Arctic clouds.

These studies are in agreement with our findings, that sea ice and snow cover significantly reduce T*. Thus, the combination of previous INP studies with the T* metric presented here demonstrates the potential influence INPs could have on the formation of MPCs in the Arctic.

When calculating T* over the Southern Ocean and separating by season (Figures 2d–2f, Table 1), it is apparent that T* is −14°C during the Austral summer (DJF) and homogeneous over the entire region. This is consistent with summertime ship measurements conducted in the Southern Ocean, where INPs were typically observed at temperatures above −14°C (McCluskey et al., 2018; Welti et al., 2020) and their concentration only varied by about one order of magnitude at −15°C (Welti et al., 2020). Meanwhile, during the Austral winter (JJA), a similar relationship between sea ice coverage and T* emerges (Figure 2e). The T* over the sea ice region drops to −27°C, while over open ocean regions the T* slightly decreases to −17°C. Consistent with the summer and winter seasons, we see that the T* values are generally cooler in the Spring than in the Fall over regions where sea ice and snow cover are slower to retreat than form (see Figure S4 in Supporting Information S1). This indicates that the sea ice acts to inhibit the emission of INPs and directly impacts cloud phase over the Southern Ocean as well. It is well known that the ocean is an important source of INPs in the Southern Ocean (Burrows et al., 2013; Schnell, 1977), which is far from the Earth's major deserts (DeMott et al., 2016; McCluskey et al., 2018). Indeed, INP observations at the remote South Pole were significantly lower than at a coastal site (Belosi et al., 2014) and increased when air mass back trajectories originated from the coast (Ardon-Dryer et al., 2011). Modeling studies have shown that replacing dust-based with marine-based INP parametrizations greatly improves the representation of clouds over the Southern Ocean (Frey & Kay, 2018; Vergara-Temprado et al., 2018). This further provides evidence that the Southern Ocean is the primary source of INPs over this region and when it is covered with sea ice, fewer INPs are emitted. Therefore, our results indicate that the decrease in T* over the sea ice is a result of the sea ice acting as a lid that inhibits the emission of INPs from the Southern Ocean and, in turn, hinders the initiation of MPCs in this region.

Previous remote sensing observations of cloud phase over the Southern Ocean have also observed a spatial pattern in the occurrence of MPCs (e.g., Mace et al., 2020; Mace et al., 2021) with a maximum in the vicinity of the so-called Antarctic Polar Front (Freeman & Lovenduski, 2016). Mace et al. (2021) attributed this relationship to potentially enhanced vertical updrafts in convective clouds over the Antarctic Polar Front due to warmer sea surface temperatures, which would loft ice crystals from lower layers of clouds to their top where a lidar-depolarization based cloud classification algorithm (Mace et al., 2020) would classify them as mixed-phase. Additionally, they highlight that these enhanced updrafts would act as a production zone for larger cloud droplets, which have been shown to be more efficient for SIP (e.g., Keinert et al., 2020; Lauber et al., 2018). Although we cannot rule out the importance of SIP on the classification of a cloud as LTMPC, through the combined use of lidar and radar observations in the 2B-CLDCLASS-LIDAR product we can reduce the importance of ice crystals being lofted to cloud top for the classification of LTMPCs. Regardless of the importance of SIP in producing ice in LTMPCs, primary ice formed on INPs is still required and thus, T* is representative of when INPs are typically involved in controlling the cloud phase over the Southern Ocean. Furthermore, when comparing T* values with the location of the Antarctic Polar Front in the summertime (see Figure 3 in Freeman & Lovenduski, 2016) there is no clear dependence, indicating that the observed seasonal variability in T* is associated with the sea ice extent and its ability to inhibit INP emissions.

With this in mind, it is important to note that there are well-documented differences in high-latitude clouds over the open ocean and sea ice due to differences in surface fluxes (e.g., heat and moisture) and thermodynamic structure (Eirund et al., 2019; Palm et al., 2010; Sotiropoulou et al., 2016; Young et al., 2017). However, to our knowledge these differences would not lead to the transition from LO to LTMPCs occurring more frequently at colder temperatures over sea ice than over open water as we observe. Furthermore, when comparing the cloud top heights and occurrence of LO and LTMPCs over the Southern Ocean (see Figure S3 in Supporting

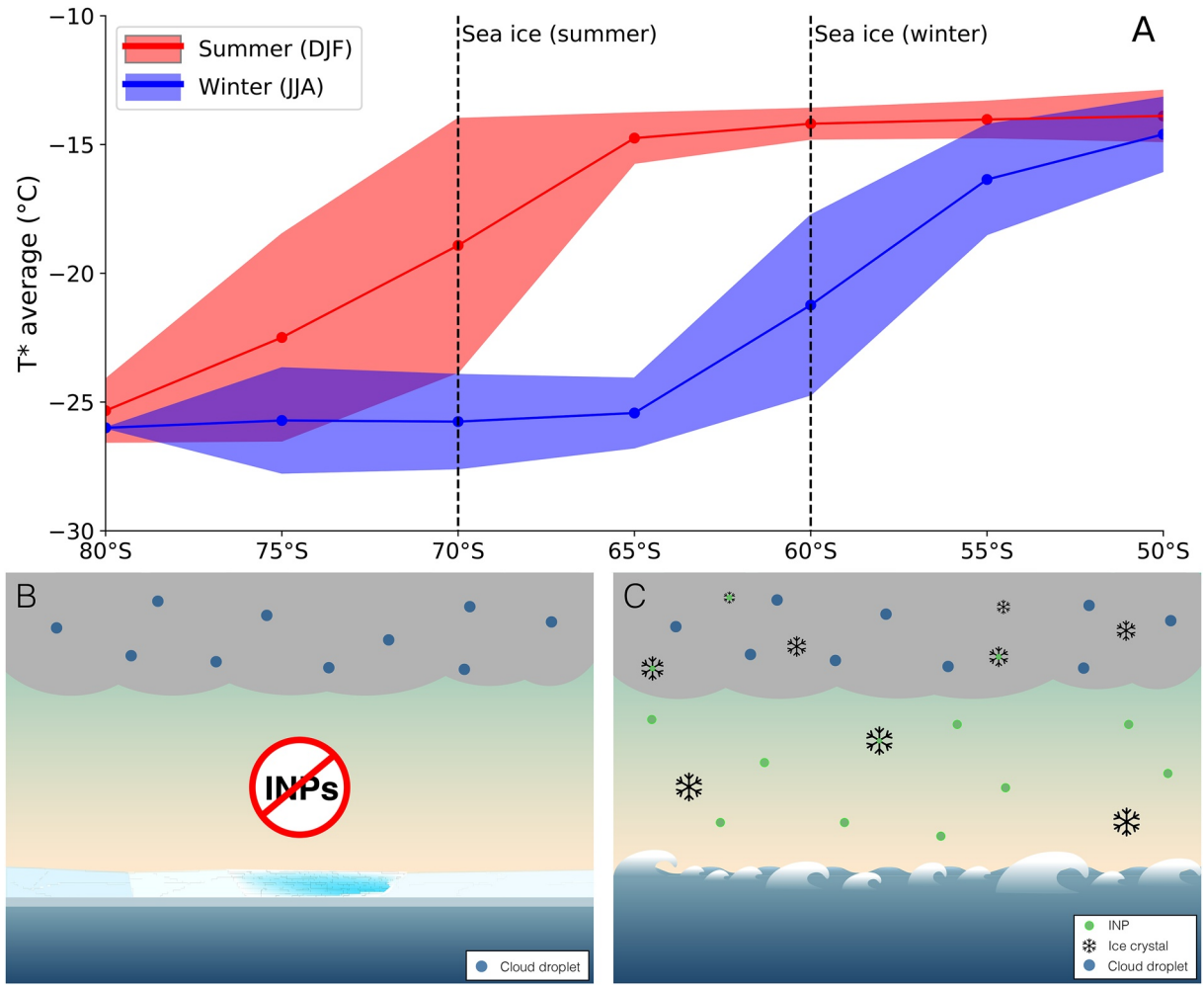

Figure 3. (a) Latitudinal average (line) and standard deviation (fill) of T* during Austral summer (red) and winter (blue) over the Southern Ocean as a northward cross section from 80°S to 50°S. (b, c) Conceptual overview of how sea ice cover influences ice-nucleating particle (INP) sources and, consequently, ice formation in mixed-phase clouds (MPCs).

Information S1), we find that they overlap and occur at the same heights in the troposphere, regardless of whether they form over open ocean or sea ice. Therefore, the observed variability in T* can be explained by the variability in the efficiency and concentration of INPs present during the onset of ice formation and MPC initiation.

4. Atmospheric Implications

The apparent relationship between the suppressed T* and sea ice and snow cover (Figure 2), which is well documented as a region with reduced INP concentrations (Bigg & Leck, 2001; Creamean et al., 2019; Wex et al., 2019), indicates that INPs play a critical role in the initiation of MPCs. Furthermore, this relationship provides additional evidence that INPs in the high-latitudes are primarily of a local origin. Without these local INP sources (due to sea ice and snow cover), only less efficient INPs (from long-range sources) are available as observable by a significantly lower T*. Ultimately, through the use of T*, we highlight the large-scale relevance of INPs on MPC formation, confirming laboratory studies dating back to the 1940s (Vonnegut, 1947) that showed the importance of INPs for MPC formation.

Based on these findings, we conclude that differing INP parametrizations are required over ice/snow-covered and ice/snow-free portions of the high-latitudes to account for the observed seasonal variations in the MPC transition temperature, T*. This is especially important for future climate projections, where in a warming climate, sea ice

and snow cover are projected to decrease (Fox-Kemper et al., 2021) and therefore, although temperatures will rise, INPs may become more abundant due to newly available source regions (i.e., ice and snow free areas).

An increase in the abundance of high-latitude INPs could have profound effects on the cloud-phase feedback (Murray et al., 2021; Prenni et al., 2007), which has so far been projected to limit warming over the Southern Ocean (Bjordal et al., 2020; Forster et al., 2021; Tan et al., 2016; Zelinka et al., 2020). The warming-induced INP increase could weaken, or even reverse, the projected increase in LO cloud occurrence with warming. This would have major implications for both the magnitude and sign of the Southern Ocean cloud feedback, thus shaping the climate evolution of the region itself and ultimately, the future climate of the entire planet. Figure 3 shows the T* averaged by latitude over the Southern Ocean. The stark contrast in T* over sea ice and open ocean indicates that in a warming world with sea ice retreat, T* over formerly ice covered regions will increase to about −15°C. As the ice covered regions currently have a T* of approximately −25°C, this would suggest that a warming of 10°C would be required to significantly offset the formation of MPCs over future ice free regions of the Southern Ocean. Therefore, without a detailed quantification of the seasonal nature of INPs in the high-latitudes and subsequent inclusion in Earth System Models, the influence of the negative cloud-phase feedback on buffering future warming will remain uncertain.

Data Availability Statement

The standard CloudSat (Stephens et al., 2002) and CALIPSO (Winker et al., 2010) data products (version R05) used in this study (2B-CLDCLASS-LIDAR, ECMWF-AUX) were downloaded from the CloudSat Data Processing Center's (at Cooperative Institute for Research in the Atmosphere, Colorado State University, Fort Collins) website (http://www.cloudsat.cira.colostate.edu).

The sea ice concentration data is from the Institute of Environmental Physics (IUP), University of Bremen, based on the ARTIST Sea Ice (ASI) algorithm (Spreen et al., 2008). The daily data sets (Melsheimer & Spreen, 2019a, 2019b, 2020a, 2020b) were downloaded for the years 2006–2017 from the data publisher PANGAEA. The dates for the Arctic and Antarctic sea ice maximum/minimum for each year were retrieved from https://www.meereisportal.de (Grosfeld et al., 2016).

The code used to analyze the satellite data and to produce the figures is available on the public GitHub repository: https://github.com/tim-carlsen/tstar-inp-satellite.git.

Acknowledgments
We gratefully acknowledge the funding by the European Research Council (ERC) through Grant StG758005. ROD would also like to acknowledge EEARO-NO-2019-0423/IceSafari, contract no. 31/2020, under the NO grants 2014–2021 of EEA Grants/Norway Grants for financial support. We would also like to thank Trude Storelvmo for her support and valuable insight throughout the development of this project and during the writing of this manuscript. Sea ice concentration data from 2006 to 2017 were obtained from https://www.meereisportal.de (Grant: REKLIM-2013-04). We would like to acknowledge the USIT statistikk service at University of Oslo and, in particular, Sahar Hassani for contributing her statistical expertise to this analysis. Many thanks to the late Dr. William Ball for his discussions and support during the development of this study. Lastly, thanks to Dr. Russ Schnell, Dr. Gesa Eirund and one anonymous reviewer for their helpful and insightful feedback on our manuscript.

References

Achtert, P., O'Connor, E. J., Brooks, I. M., Sotiropoulou, G., Shupe, M. D., Pospichal, B., et al. (2020). Properties of Arctic liquid and mixed-phase clouds from shipborne cloudnet observations during ACSE 2014. *Atmospheric Chemistry and Physics*, *20*(23), 14983–15002. https://doi.org/10.5194/acp-20-14983-2020

Ardon-Dryer, K., Levin, Z., & Lawson, R. P. (2011). Characteristics of immersion freezing nuclei at the south pole station in Antarctica. *Atmospheric Chemistry and Physics*, *11*(8), 4015–4024. https://doi.org/10.5194/acp-11-4015-2011

Atkinson, J., Murray, B., Woodhouse, M., Whale, T., Baustian, K., Carslaw, K., et al. (2013). The importance of feldspar for ice nucleation by mineral dust in mixed-phase clouds. *Nature*, *498*(7454), 355–358. https://doi.org/10.1038/nature12278

Belosi, F., Santachiara, G., & Prodi, F. (2014). Ice-forming nuclei in Antarctica: New and past measurements. *Atmospheric Research*, *145–146*, 105–111. https://doi.org/10.1016/j.atmosres.2014.03.030

Bigg, E. K. (1996). Ice forming nuclei in the high arctic. *Tellus B: Chemical and Physical Meteorology*, *48*(2), 223–233. https://doi.org/10.3402/tellusb.v48i2.15888

Bigg, E. K., & Leck, C. (2001). Properties of the aerosol over the central Arctic Ocean. *Journal of Geophysical Research*, *106*(D23), 32101–32109. https://doi.org/10.1029/1999JD901136

Bjordal, J., Storelvmo, T., Alterskjær, K., & Carlsen, T. (2020). Equilibrium climate sensitivity above 5°C plausible due to state-dependent cloud feedback. *Nature Geoscience*, *13*(11), 718–721. https://doi.org/10.1038/s41561-020-00649-1

Boose, Y., Sierau, B., García, M. I., Rodríguez, S., Alastuey, A., Linke, C., et al. (2016). Ice nucleating particles in the Saharan Air Layer. *Atmospheric Chemistry and Physics*, *16*(14), 9067–9087. https://doi.org/10.5194/acp-16-9067-2016

Borys, R. D. (1983). *The effects of long range transport of air pollutants on arctic cloud active aerosol (The effects of long range transport of air pollutants on Arctic cloud active aerosol, Atmos. Sci. (paper no. 367))*. Department of Atmospheric Science Colorado State University, Ft. Collins.

Borys, R. D. (1989). Studies of ice nucleation by Arctic aerosol on AGASP-II. *Journal of Atmospheric Chemistry*, *9*(1–3), 169–185. https://doi.org/10.1007/bf00052831

Burrows, S. M., Hoose, C., Pöschl, U., & Lawrence, M. G. (2013). Ice nuclei in marine air: Biogenic particles or dust? *Atmospheric Chemistry and Physics*, *13*(1), 245–267. https://doi.org/10.5194/acp-13-245-2013

Cantrell, W., & Heymsfield, A. (2005). Production of ice in tropospheric clouds: A review. *Bulletin of the American Meteorological Society*, *86*(6), 795–808. https://doi.org/10.1175/BAMS-86-6-795

Choi, Y.-S., Lindzen, R. S., Ho, C.-H., & Kim, J. (2010). Space observations of cold-cloud phase change. *Proceedings of the National Academy of Sciences*, *107*(25), 11211–11216. https://doi.org/10.1073/pnas.1006241107

Costa, A., Meyer, J., Afchine, A., Luebke, A., Günther, G., Dorsey, J. R., et al. (2017). Classification of arctic, midlatitude and tropical clouds in the mixed-phase temperature regime. *Atmospheric Chemistry and Physics*, *17*(19), 12219–12238. https://doi.org/10.5194/acp-17-12219-2017

Creamean, J. M., Cross, J. N., Pickart, R., McRaven, L., Lin, P., Pacini, A., et al. (2019). Ice nucleating particles carried from below a phytoplankton bloom to the arctic atmosphere. *Geophysical Research Letters*, *46*(14), 8572–8581. https://doi.org/10.1029/2019GL083039

Creamean, J. M., Kirpes, R. M., Pratt, K. A., Spada, N. J., Maahn, M., de Boer, G., et al. (2018). Marine and terrestrial influences on ice nucleating particles during continuous springtime measurements in an arctic oilfield location. *Atmospheric Chemistry and Physics*, *18*(24), 18023–18042. https://doi.org/10.5194/acp-18-18023-2018

Curry, J. A., Hobbs, P. V., King, M. D., Randall, D. A., Minnis, P., Isaac, G. A., et al. (2000). Fire arctic clouds experiment. *Bulletin of the American Meteorological Society*, *81*(1), 5–30. https://doi.org/10.1175/1520-0477(2000)081<0005:FACE>2.3.CO;2

de Boer, G., Hashino, T., & Tripoli, G. J. (2010). Ice nucleation through immersion freezing in mixed-phase stratiform clouds: Theory and numerical simulations. *Atmospheric Research*, *96*(2), 315–324. https://doi.org/10.1016/j.atmosres.2009.09.012

DeMott, P. J., Hill, T. C. J., McCluskey, C. S., Prather, K. A., Collins, D. B., Sullivan, R. C., et al. (2016). Sea spray aerosol as a unique source of ice nucleating particles. *Proceedings of the National Academy of Sciences*, *113*(21), 5797–5803. https://doi.org/10.1073/pnas.1514034112

DeMott, P. J., Prenni, A. J., Liu, X., Kreidenweis, S. M., Petters, M. D., Twohy, C. H., et al. (2010). Predicting global atmospheric ice nuclei distributions and their impacts on climate. *Proceedings of the National Academy of Sciences*, *107*(25), 11217–11222. https://doi.org/10.1073/pnas.0910818107

Eirund, G. K., Possner, A., & Lohmann, U. (2019). Response of arctic mixed-phase clouds to aerosol perturbations under different surface forcings. *Atmospheric Chemistry and Physics*, *19*(15), 9847–9864. https://doi.org/10.5194/acp-19-9847-2019

Engelmann, R., Ansmann, A., Ohneiser, K., Griesche, H., Radenz, M., Hofer, J., et al. (2021). Wildfire smoke, arctic haze, and aerosol effects on mixed-phase and cirrus clouds over the north pole region during mosaic: An introduction. *Atmospheric Chemistry and Physics*, *21*(17), 13397–13423. https://doi.org/10.5194/acp-21-13397-2021

Fletcher, N. H. (1962). *The physics of rainclouds*. Cambridge University Press.

Forster, P., Storelvmo, T., Armour, K., Collins, W., Dufresne, J.-L., Frame, D., et al. (Eds.). In *Climate Change 2021: The Physical Science Basis. Contribution of working Group I to the Sixth assessment report of the intergovernmental panel on climate Change*. Cambridge University Press.

Fountain, A. G., & Ohtake, T. (1985). Concentrations and source areas of ice nuclei in the Alaskan atmosphere. *Journal of Applied Meteorology and Climatology*, *24*(4), 377–382. https://doi.org/10.1175/1520-0450(1985)024<0377:CASAOI>2.0.CO;2

Fox-Kemper, B., Hewitt, H. T., Xiao, C., Aalgeirsdóttir, G., Drijfhout, S. S., Edwards, T. L., et al. (Eds.). *Climate Change 2021: The Physical Science Basis. Contribution of working Group I to the Sixth assessment report of the intergovernmental panel on climate Change*. Cambridge University Press.

Freeman, N. M., & Lovenduski, N. S. (2016). Mapping the Antarctic polar front: Weekly realizations from 2002 to 2014. *Earth System Science Data*, *8*(1), 191–198. https://doi.org/10.5194/essd-8-191-2016

Frey, W. R., & Kay, J. E. (2018). The influence of extratropical cloud phase and amount feedbacks on climate sensitivity. *Climate Dynamics*, *50*(7–8), 3097–3116. https://doi.org/10.1007/s00382-017-3796-5

Griesche, H. J., Ohneiser, K., Seifert, P., Radenz, M., Engelmann, R., & Ansmann, A. (2021). Contrasting ice formation in arctic clouds: Surface-coupled vs. surface-decoupled clouds. *Atmospheric Chemistry and Physics*, *21*(13), 10357–10374. https://doi.org/10.5194/acp-21-10357-2021

Grosfeld, K., Treffeisen, R., Asseng, J., Bartsch, A., Bräuer, B., Fritzsch, B., et al. (2016). *Online sea-ice knowledge and data platform www.meereisportal.de* (Vol. 85). Alfred Wegener Institute for Polar and Marine Research & German Society of Polar Research. https://doi.org/10.2312/polfor.2016.011.2

Guy, H., Brooks, I. M., Carslaw, K. S., Murray, B. J., Walden, V. P., Shupe, M. D., et al. (2021). Controls on surface aerosol particle number concentrations and aerosol-limited cloud regimes over the central Greenland ice sheet. *Atmospheric Chemistry and Physics*, *21*(19), 15351–15374. https://doi.org/10.5194/acp-21-15351-2021

Hallett, J., & Mossop, S. C. (1974). Production of secondary ice particles during the riming process. *Nature*, *249*(5452), 26–28. https://doi.org/10.1038/249026a0

Hartmann, M., Adachi, K., Eppers, O., Haas, C., Herber, A., Holzinger, R., et al. (2020). Wintertime airborne measurements of ice nucleating particles in the high arctic: A hint to a marine, biogenic source for ice nucleating particles. *Geophysical Research Letters*, *47*(13), e2020GL087770. https://doi.org/10.1029/2020GL087770

Irish, V. E., Hanna, S. J., Xi, Y., Boyer, M., Polishchuk, E., Ahmed, M., et al. (2019). Revisiting properties and concentrations of ice-nucleating particles in the sea surface microlayer and bulk seawater in the Canadian Arctic during summer. *Atmospheric Chemistry and Physics*, *19*(11), 7775–7787. https://doi.org/10.5194/acp-19-7775-2019

Kanji, Z. A., Ladino, L. A., Wex, H., Boose, Y., Burkert-Kohn, M., Cziczo, D. J., & Krämer, M. (2017). Overview of ice nucleating particles. *Meteorological Monographs*, *58*, 11–133. https://doi.org/10.1175/AMSMONOGRAPHS-D-16-0006.1

Keinert, A., Spannagel, D., Leisner, T., & Kiselev, A. (2020). Secondary ice production upon freezing of freely falling drizzle droplets. *Journal of the Atmospheric Sciences*, *77*(8), 2959–2967. https://doi.org/10.1175/JAS-D-20-0081.1

Korolev, A. (2007). Limitations of the Wegener–Bergeron–Findeisen mechanism in the evolution of mixed-phase clouds. *Journal of the Atmospheric Sciences*, *64*(9), 3372–3375. https://doi.org/10.1175/JAS4035.1

Korolev, A., Heckman, I., Wolde, M., Ackerman, A. S., Fridlind, A. M., Ladino, L. A., et al. (2020). A new look at the environmental conditions favorable to secondary ice production. *Atmospheric Chemistry and Physics*, *20*(3), 1391–1429. https://doi.org/10.5194/acp-20-1391-2020

Korolev, A., & Leisner, T. (2020). Review of experimental studies of secondary ice production. *Atmospheric Chemistry and Physics*, *20*(20), 11767–11797. https://doi.org/10.5194/acp-20-11767-2020

Korolev, A., McFarquhar, G., Field, P. R., Franklin, C., Lawson, P., Wang, Z., et al. (2017). Mixed-phase clouds: Progress and challenges. *Meteorological Monographs*, *58*, 51–550. https://doi.org/10.1175/AMSMONOGRAPHS-D-17-0001.1

Lacher, L., DeMott, P. J., Levin, E. J. T., Suski, K. J., Boose, Y., Zipori, A., et al. (2018). Background free-tropospheric ice nucleating particle concentrations at mixed-phase cloud conditions. *Journal of Geophysical Research: Atmospheres*, *123*(18), 10506–10525. https://doi.org/10.1029/2018JD028338

Lacher, L., Lohmann, U., Boose, Y., Zipori, A., Herrmann, E., Bukowiecki, N., et al. (2017). The horizontal ice nucleation chamber (HINC): INP measurements at conditions relevant for mixed-phase clouds at the high altitude research station Jungfraujoch. *Atmospheric Chemistry and Physics*, *17*(24), 15199–15224. https://doi.org/10.5194/acp-17-15199-2017

Ladino, L. A., Korolev, A., Heckman, I., Wolde, M., Fridlind, A. M., & Ackerman, A. S. (2017). On the role of ice-nucleating aerosol in the formation of ice particles in tropical mesoscale convective systems. *Geophysical Research Letters*, *44*(3), 1574–1582. https://doi.org/10.1002/2016GL072455

Lauber, A., Kiselev, A., Pander, T., Handmann, P., & Leisner, T. (2018). Secondary ice formation during freezing of levitated droplets. *Journal of the Atmospheric Sciences*, *75*(8), 2815–2826. https://doi.org/10.1175/JAS-D-18-0052.1

Lawson, R. P., Woods, S., & Morrison, H. (2015). The microphysics of ice and precipitation development in tropical cumulus clouds. *Journal of the Atmospheric Sciences*, *72*(6), 2429–2445. https://doi.org/10.1175/jas-d-14-0274.1

Mace, G. G., Benson, S., & Hu, Y. (2020). On the frequency of occurrence of the ice phase in supercooled southern ocean low clouds derived from CALIPSO and CloudSat. *Geophysical Research Letters*, *47*(14), e2020GL087554. https://doi.org/10.1029/2020GL087554

Mace, G. G., Protat, A., & Benson, S. (2021). Mixed-phase clouds over the southern ocean as observed from satellite and surface based lidar and radar. *Journal of Geophysical Research: Atmospheres*, *126*(16), e2021JD034569. https://doi.org/10.1029/2021JD034569

McCluskey, C. S., Hill, T. C. J., Humphries, R. S., Rauker, A. M., Moreau, S., Strutton, P. G., et al. (2018). Observations of ice nucleating particles over southern ocean waters. *Geophysical Research Letters*, *45*(21), 11989–11997. https://doi.org/10.1029/2018GL079981

McCluskey, C. S., Ovadnevaite, J., Rinaldi, M., Atkinson, J., Belosi, F., Ceburnis, D., et al. (2018). Marine and terrestrial organic ice-nucleating particles in pristine marine to continentally influenced northeast Atlantic air masses. *Journal of Geophysical Research: Atmospheres*, *123*(11), 6196–6212. https://doi.org/10.1029/2017JD028033

Melsheimer, C., & Spreen, G. (2019a). AMSR2 ASI sea ice concentration data, Antarctic, version 5.4 (NetCDF) (July 2012–December 2019) [data set]. PANGAEA. https://doi.org/10.1594/PANGAEA.898400

Melsheimer, C., & Spreen, G. (2019b). AMSR2 ASI sea ice concentration data, Arctic, version 5.4 (NetCDF) (July 2012–December 2019) [data set]. PANGAEA. https://doi.org/10.1594/PANGAEA.898399

Melsheimer, C., & Spreen, G. (2020a). AMSR-E ASI sea ice concentration data, Antarctic, version 5.4 (NetCDF) (June 2002–September 2011) [data set]. PANGAEA. https://doi.org/10.1594/PANGAEA.919778

Melsheimer, C., & Spreen, G. (2020b). AMSR-E ASI sea ice concentration data, Arctic, version 5.4 (NetCDF) (June 2002–September 2011) [data set]. PANGAEA. https://doi.org/10.1594/PANGAEA.919777

Meyers, M. P., DeMott, P. J., & Cotton, W. R. (1992). New primary ice-nucleation parameterizations in an explicit cloud model. *Journal of Applied Meteorology and Climatology*, *31*(7), 708–721. https://doi.org/10.1175/1520-0450(1992)031<0708:NPINPI>2.0.CO;2

Mignani, C., Creamean, J. M., Zimmermann, L., Alewell, C., & Conen, F. (2019). New type of evidence for secondary ice formation at around −5c in mixed-phase clouds. *Atmospheric Chemistry and Physics*, *19*(2), 877–886. https://doi.org/10.5194/acp-19-877-2019

Morrison, H., De Boer, G., Feingold, G., Harrington, J., Shupe, M., & Sulia, K. (2012). Resilience of persistent arctic mixed-phase clouds. *Nature Geoscience*, *5*(1), 11–17. https://doi.org/10.1038/ngeo1332

Murray, B. J., Carslaw, K. S., & Field, P. R. (2021). Opinion: Cloud-phase climate feedback and the importance of ice-nucleating particles. *Atmospheric Chemistry and Physics*, *21*(2), 665–679. https://doi.org/10.5194/acp-21-665-2021

Murray, B. J., O'Sullivan, D., Atkinson, J. D., & Webb, M. E. (2012). Ice nucleation by particles immersed in supercooled cloud droplets. *Chemical Society Reviews*, *41*(19), 6519–6554. https://doi.org/10.1039/C2CS35200A

Palm, S. P., Strey, S. T., Spinhirne, J., & Markus, T. (2010). Influence of Arctic sea ice extent on polar cloud fraction and vertical structure and implications for regional climate. *Journal of Geophysical Research*, *115*(D21), D21209. https://doi.org/10.1029/2010JD013900

Petters, M. D., & Wright, T. P. (2015). Revisiting ice nucleation from precipitation samples. *Geophysical Research Letters*, *42*(20), 8758–8766. https://doi.org/10.1002/2015GL065733

Pithan, F., Svensson, G., Caballero, R., Chechin, D., Cronin, T. W., Ekman, A. M. L., et al. (2018). Role of air-mass transformations in exchange between the arctic and mid-latitudes. *Nature Geoscience*, *11*(11), 805–812. https://doi.org/10.1038/s41561-018-0234-1

Pratt, K., DeMott, P., French, J., Wang, Z., Westphal, D., Heymsfield, A., et al. (2009). In situ detection of biological particles in cloud ice-crystals. *Nature Geoscience*, *2*(6), 398–401. https://doi.org/10.1038/NGEO521

Prenni, A. J., Harrington, J. Y., Tjernström, M., DeMott, P. J., Avramov, A., Long, C. N., et al. (2007). Can ice-nucleating aerosols affect arctic seasonal climate? *Bulletin of the American Meteorological Society*, *88*(4), 541–550. https://doi.org/10.1175/BAMS-88-4-541

Ramelli, F., Henneberger, J., David, R. O., Bühl, J., Radenz, M., Seifert, P., et al. (2021). Microphysical investigation of the seeder and feeder region of an alpine mixed-phase cloud. *Atmospheric Chemistry and Physics*, *21*(9), 6681–6706. https://doi.org/10.5194/acp-21-6681-2021

Rangno, A. L., & Hobbs, P. V. (2001). Ice particles in stratiform clouds in the arctic and possible mechanisms for the production of high ice concentrations. *Journal of Geophysical Research*, *106*(D14), 15065–15075. https://doi.org/10.1029/2000JD900286

Rogers, D. C., DeMott, P. J., & Kreidenweis, S. M. (2001). Airborne measurements of tropospheric ice-nucleating aerosol particles in the arctic spring. *Journal of Geophysical Research*, *106*(D14), 15053–15063. https://doi.org/10.1029/2000JD900790

Sassen, K., Wang, Z., & Liu, D. (2008). Global distribution of cirrus clouds from cloudsat/cloud-aerosol lidar and infrared pathfinder satellite observations (CALIPSO) measurements. *Journal of Geophysical Research*, *113*(D8), D00A12. https://doi.org/10.1029/2008JD009972

Schneider, J., Höhler, K., Heikkilä, P., Keskinen, J., Bertozzi, B., Bogert, P., et al. (2021). The seasonal cycle of ice-nucleating particles linked to the abundance of biogenic aerosol in boreal forests. *Atmospheric Chemistry and Physics*, *21*(5), 3899–3918. https://doi.org/10.5194/acp-21-3899-2021

Schnell, R. C. (1977). Ice nuclei in seawater, fog water and marine air off the coast of nova scotia: Summer 1975. *Journal of the Atmospheric Sciences*, *34*(8), 1299–1305. https://doi.org/10.1175/1520-0469(1977)034<1299:INISFW>2.0.CO;2

Schnell, R. C., & Vali, G. (1975). Freezing nuclei in marine waters. *Tellus*, *27*(3), 321–323. https://doi.org/10.3402/tellusa.v27i3.9911

Sotiropoulou, G., Tjernström, M., Sedlar, J., Achtert, P., Brooks, B. J., Brooks, I. M., et al. (2016). Atmospheric conditions during the arctic clouds in summer experiment (ACSE): Contrasting open water and sea ice surfaces during melt and freeze-up seasons. *Journal of Climate*, *29*(24), 8721–8744. https://doi.org/10.1175/JCLI-D-16-0211.1

Spreen, G., Kaleschke, L., & Heygster, G. (2008). Sea ice remote sensing using AMSR-E 89-GHz channels. *Journal of Geophysical Research*, *113*(C2), C02S03. https://doi.org/10.1029/2005JC003384

Stephens, G. L., Vane, D. G., Boain, R. J., Mace, G. G., Sassen, K., Wang, Z., et al. (2002). The cloudsat mission and the a-train: A new dimension of space-based observations of clouds and precipitation. *Bulletin of the American Meteorological Society*, *83*(12), 1771–1790. https://doi.org/10.1175/BAMS-83-12-1771

Stopelli, E., Conen, F., Morris, C., Herrmann, E., Bukowiecki, N., & Alewell, C. (2015). Ice nucleation active particles are efficiently removed by precipitating clouds. *Scientific Reports*, *5*(1), 16433. https://doi.org/10.1038/srep16433

Tan, I., Storelvmo, T., & Choi, Y.-S. (2014). Spaceborne lidar observations of the ice-nucleating potential of dust, polluted dust, and smoke aerosols in mixed-phase clouds. *Journal of Geophysical Research: Atmospheres*, *119*(11), 6653–6665. https://doi.org/10.1002/2013JD021333

Tan, I., Storelvmo, T., & Zelinka, M. D. (2016). Observational constraints on mixed-phase clouds imply higher climate sensitivity. *Science*, *352*(6282), 224–227. https://doi.org/10.1126/science.aad5300

Tobo, Y., Adachi, K., DeMott, P., Hill, T., Hamilton, D., Mahowald, N., et al. (2019). Glacially sourced dust as a potentially significant source of ice nucleating particles. *Nature Geoscience*, *12*(4), 1–6. https://doi.org/10.1038/s41561-019-0314-x

Vali, G. (1971). Supercooling of water and nucleation of ice (drop freezer). *American Journal of Physics*, *39*(10), 1125–1128. https://doi.org/10.1119/1.1976585

Vergara-Temprado, J., Miltenberger, A. K., Furtado, K., Grosvenor, D. P., Shipway, B. J., Hill, A. A., et al. (2018). Strong control of southern ocean cloud reflectivity by ice-nucleating particles. *Proceedings of the National Academy of Sciences*, *115*(11), 2687–2692. https://doi.org/10.1073/pnas.1721627115

Vonnegut, B. (1947). The nucleation of ice formation by silver iodide. *Journal of Applied Physics*, *18*(7), 593–595. https://doi.org/10.1063/1.1697813

Wang, Z. (2019). Cloudsat 2b-cldclass-lidar product process description and interface control document. *[Computer software manual]* .

Welti, A., Bigg, E. K., DeMott, P. J., Gong, X., Hartmann, M., Harvey, M., et al. (2020). Ship-based measurements of ice nuclei concentrations over the Arctic, Atlantic, Pacific and Southern Oceans. *Atmospheric Chemistry and Physics*, *20*(23), 15191–15206. https://doi.org/10.5194/acp-20-15191-2020

Westbrook, C. D., & Illingworth, A. J. (2013). The formation of ice in a long-lived supercooled layer cloud. *Quarterly Journal of the Royal Meteorological Society*, *139*(677), 2209–2221. https://doi.org/10.1002/qj.2096

Wex, H., Huang, L., Zhang, W., Hung, H., Traversi, R., Becagli, S., et al. (2019). Annual variability of ice-nucleating particle concentrations at different arctic locations. *Atmospheric Chemistry and Physics*, *19*(7), 5293–5311. https://doi.org/10.5194/acp-19-5293-2019

Wilson, T., Ladino, L., Alpert, P., Breckels, M., Brooks, I., Browse, J., et al. (2015). A marine biogenic source of atmospheric ice-nucleating particles. *Nature*, *525*(7568), 234–238. https://doi.org/10.1038/nature14986

Winker, D. M., Hunt, W. H., & McGill, M. J. (2007). Initial performance assessment of CALIOP. *Geophysical Research Letters*, *34*(19), L19803. https://doi.org/10.1029/2007GL030135

Winker, D. M., Pelon, J., Coakley, J. A., Ackerman, S. A., Charlson, R. J., Colarco, P. R., et al. (2010). The CALIPSO mission: A global 3d view of aerosols and clouds. *Bulletin of the American Meteorological Society*, *91*(9), 1211–1230. https://doi.org/10.1175/2010BAMS3009.1

Young, G., Connolly, P. J., Jones, H. M., & Choularton, T. W. (2017). Microphysical sensitivity of coupled springtime arctic stratocumulus to modelled primary ice over the ice pack, marginal ice, and ocean. *Atmospheric Chemistry and Physics*, *17*(6), 4209–4227. https://doi.org/10.5194/acp-17-4209-2017

Zelinka, M. D., Myers, T. A., McCoy, D. T., Po-Chedley, S., Caldwell, P. M., Ceppi, P., et al. (2020). Causes of higher climate sensitivity in CMIP6 models. *Geophysical Research Letters*, *47*(1), e2019GL085782. https://doi.org/10.1029/2019GL085782

Zhang, D., Wang, Z., & Liu, D. (2010). A global view of midlevel liquid-layer topped stratiform cloud distribution and phase partition from CALIPSO and CloudSat measurements. *Journal of Geophysical Research*, *115*(D4), D00H13. https://doi.org/10.1029/2009JD012143